Nuclear Engineering and Design 420 (2024) 113018

Contents lists available at ScienceDirect

Nuclear Engineering and Design

journal homepage: www.elsevier.com/locate/nucengdes

# Scaling-up assessment of natural circulation phenomena in integral Small Modular Reactor by TRACE code

Fulvio Mascari [a,*], Andrea Bersano [a,*], Brian G. Woods [b], Jose N. Reyes [c], Kent Welter [c], Hideo Nakamura [d]

[a] FSN-SICNUC, ENEA C.R. Bologna, Via Martiri di Monte Sole 4, 40129 Bologna, Italy
[b] Department of Nuclear Engineering and Radiation Health Physics, Oregon State University, 128 Radiation Center, Corvallis, OR 97331-5902, USA
[c] NuScale Power, 1100 NE Circle Blvd., Corvallis, OR 97330, USA
[d] JAEA, Shirakata, Tokai, Ibaraki 319-1195 Japan

ARTICLE INFO

*Keywords:*
Scaling
Natural circulation
TRACE
OSU-MASLWR

ABSTRACT

Small Modular Reactors (SMRs) adopting passive mitigation strategies are currently the most promising technology for the near term deployment of nuclear power generation. Different SMRs designs are currently under development and are, in general, characterized by some common features with the current reactors and by other features typical of their designs. Therefore, though numerous code validation study against natural circulation (NC) have been performed for large scale reactors, further analyses are necessary to characterize the capability of codes against available experimental data representative of SMR phenomenology. Though different scaling methodologies have been developed, considering the complex geometry and phenomena of a NPP, in the design of scaled-down experimental facilities it is not possible to avoid distortions, which should be limited to non-dominant phenomena. Even if dominant phenomena are preserved, due to the missing data at NPP scale, the code accuracy should be tested at different scales. Therefore, in a verification and validation process, the uncertainty related to the code scaling-up capability should be addressed, for example using counter-part tests. Since NC tests at different scales in integral test facilities devoted to SMR are currently not available, a numerical scaling methodology is here proposed. Based on previous activities, having as a reference the NC DOE tests developed in the OSU-MASLWR facility, the USNRC best estimate thermal hydraulic TRACE code has been validated for simulating NC in steady and transient conditions. Since the OSU-MASLWR is volume and height scaled, the target of this paper is to assess the scaling-up capability of the OSU-MASLWR Reactor Pressure Vessel nodalization in the prediction at different scales of NC and other phenomena typical of SMR, having as a base the OSU-MASLWR-002 single phase NC data. This, also, gives some first insights about the TRACE scaling-up capability against single-phase NC in integral type configurations.

## 1. Introduction

The OSU-MASLWR is a scaled-down Integral Test Facility (ITF) (Modro et al., 2003; Reyes and King, 2003; Reyes et al., 2007; Reyes, 2005; Mascari et al., 2012c; Mascari et al., 2016; OECD/NEA/CSNI, 2017; Mascari et al., 2008; Mascari et al., 2011a; Mascari et al., 2011b; Mascari et al., 2012a; Mascari et al., 2012b; Mascari et al., 2019; Mascari et al., 2023) built at Oregon State University (OSU) to thermal-hydraulically characterize the phenomena typical of the Multi-Application Small Light Water Reactor (MASLWR) design. The MASLWR is a Small Modular Reactor (SMR) relying on natural circulation during both steady state and transient conditions. It has a compact helical coil Steam Generator (SG) and the pressurizer located inside the Reactor Pressure Vessel (RPV). The experimental data produced in the OSU-MASLWR facility are useful for the assessment of the computational tools necessary for deterministic safety analysis. It should be noted that the MASLWR is the base for the NuScale SMR design.

In the past, to support the independent vendor review of Light Water Reactor (LWR) designs, the U.S. Nuclear Regulatory Commission (USNRC) maintained four distinct computer codes (RAMONA, the RELAP5, the TRAC-B and the TRAC-P). These codes were adopted to analyze the system thermal hydraulic response. Over more than the last 20 years, the USNRC has developed an advanced best estimate

* Corresponding authors.
*E-mail addresses:* fulvio.mascari@enea.it (F. Mascari), andrea.bersano@enea.it (A. Bersano).

https://doi.org/10.1016/j.nucengdes.2024.113018
Received 19 December 2023; Received in revised form 9 February 2024; Accepted 10 February 2024
Available online 13 February 2024

**Nomenclature**

| | |
|---|---|
| AA | Average Amplitude |
| ADS | Automatic Depressurization System |
| BASE | Base OSU-MASLWR input deck/calculation |
| CPV | Cooling Pool Vessel |
| FFTBM | Fast Fourier Transform Based Method |
| FW | Feed Water |
| HPC | High Pressure Containment |
| ICSP | International Collaborative Standard Problem |
| ITF | Integral Test Facility |
| KH | Height scaled OSU-MASLWR input deck/calculation |
| KV | Volume scaled OSU-MASLWR input deck/calculation |
| LWR | Light Water Reactor |
| MASLWR | Multi-Application Small Light Water Reactor |
| OSU | Oregon State University |
| PhW | Phenomenological Windows |
| RPV | Reactor Pressure Vessel |
| SG | Steam Generator |
| SMR | Small Modular Reactor |
| SNAP | Symbolic Nuclear Analysis Package |
| TRACE | TRAC/RELAP Advanced Computational Engine |
| USNRC | US Nuclear Regulatory Commission |
| WF | Weighted Frequency |

thermal–hydraulic system code, by merging, among other things, the capabilities of the previous codes into one. This new code is called TRAC/RELAP Advanced Computational Engine (TRACE) (U. S. Nuclear Regulatory Commission, 2013), and it is a component-oriented code designed to perform best estimate analyses for LWR. In particular, TRACE is developed to simulate operational transients, Loss Of Coolant Accidents (LOCA), other transient typical of LWRs and to model the thermal–hydraulic phenomena taking place in the experimental facilities used to study the steady state and transient behavior of reactor systems (Mascari et al., 2016).

The TRACE code has been extensively validated in the past against the experimental data collected in the OSU-MASLWR facility, both considering natural circulation and primary/containment coupling phenomena (Mascari et al., 2016; Mascari et al., 2008; Mascari et al., 2011a; Mascari et al., 2011b; Mascari et al., 2012a; Mascari et al., 2012b; Mascari et al., 2019; IAEA, 2014). Considering natural circulation, which is the main objective of this analysis, OSU-MASLWR tests 002 and 003A and IAEA International Collaborative Standard Problem (ICSP) SP-3 are particularly relevant. The validation of TRACE code against the OSU-MASLWR tests 002 (natural circulation at core power up to 210 kW) has been presented in previous references. In particular, in (Mascari et al., 2008) a first analysis has been presented with a sensitivity analysis on some relevant model parameters (e.g. heat losses, secondary side heat transfer diameter, etc.). Moreover, in (Mascari et al., 2011b) a sensitivity analysis on the helical coil SG has been carried out. In (Mascari et al., 2016) it has been shown that the use of flow Reynolds number-dependent loss coefficient, available from TRACE V5.0 patch 3, improves the prediction of the primary flow rate. Finally, in (Mascari et al., 2019) it has been shown the improvements in the prediction of the SG behavior adopting the “Curved Pipe” option, available from TRACE V5.0 patch 4. For the OSU-MASLWR tests 003A (natural circulation at core power of 210 kW), the validation of TRACE code has been presented in (Mascari et al., 2012a). For the ICSP SP-3 test (power maneuvering), in (Mascari et al., 2011a) it is presented the TRACE V5.0 patch 01 calculated data developed during the double-blind phase of the ICSP. In addition, IAEA TECDOC-1733 (IAEA, 2014) collects the complete results of the ICSP. Moreover, in (Chung et al., 2014) the data have been also used for the validation of the TASS/SMR code.

Considering that the data obtained from scaled ITF experiments are not directly applicable to full-scale conditions due to scale distortions (OECD/NEA/CSNI, 2017), validated computational codes should be adopted as extrapolation tools (Mascari et al., 2015). An approach called Kv-scaling is a procedure for system code simulation in which well-defined (measured) scaled ITF are converted to an NPP nodalization, and the test is simulated with this nodalization (OECD/NEA/CSNI, 2017). Several Kv scaled calculations have been performed in the past for different reactor designs and accident scenarios. One first application of Kv scaled calculation was presented in (Bovalini et al., 1992) for a BWR small break LOCA scenario with the RELAP5/mod2 code based on three ITF data sets. In (D’Auria, 1992) a scaling analysis was performed for one scenario in a BWR and three scenarios in a PWR. Then in (D’Auria et al., 1993) a loss of feedwater scenario in a PWR was analyzed adopting the RELAP5/mod3 code based on experimental data developed from two ITF data sets. The adoption of Kv scaled calculations was then included in the Uncertainty Methodology Based on Accuracy Extrapolation (UMAE) (D’Auria et al., 1995). More recently, a Kv scaled calculation was presented in (D’Auria et al., 2005) to compare the behavior of PWR and VVER1000 ITF in a small break LOCA scenario and in (Reventós et al., 2007) as a step for the qualification of nuclear power plant nodalizations. Kv scaled calculations have also been performed to create hybrid code models used to explain the distortions that may appear in the comparison of full plant simulations with scaled-up ITF data (Reventos et al., 2019). More details on Kv scaled calculations and additional references can be found in (OECD/NEA/CSNI, 2017).

Having as a base the validation of the TRACE code against natural circulation phenomena and taking into account that the OSU-MASLWR facility is scaled-down (1:3 in length and 1:254.7 in volume), the aim of this activity is to show the scalability of the input-deck developed for the TRACE code. The scale-up has been performed in two subsequent steps: length scaling and flow area scaling to obtain the final volume scaling. The natural circulation test 002 is considered in the present analysis. Both the original OSU-MASLWR and scaled-up nodalizations have been developed through the graphical user interface Symbolic Nuclear Analysis Package (SNAP) (Applied Programming Technology, Inc., 2021). In addition, this activity gives some first insights about the scaling-up capability of the TRACE code against natural circulation in integral type systems.

To evaluate the scaling results, relevant thermal–hydraulic parameters and characteristic and non-dimensional numbers have been developed. The accuracy of the base calculation (BASE), of the height scaled calculation (KH) and volume scaled calculation (KV) have been evaluated both from a qualitative and quantitative point of view (Mascari et al., 2015). For the quantitative accuracy evaluation and to compare the characteristic and non-dimensional numbers resulting from the three calculations, the Fast Fourier Transform Based Method (FFTBM) has been applied (Ambrosini et al., 1990). In (Mascari et al., 2022) the preliminary results of the analysis have been presented; this derived paper collects the complete results.

## 2. Description of OSU-MASLWR facility and test 002

### 2.1. OSU-MASLWR test facility

The OSU-MASLWR test facility is scaled at 1:3 length scale, 1:254.7 vol scale and 1:1 time scale. The scaling of the facility was performed adopting the Hierarchical Two-Tiered Scaling (H2TS) method (Reyes and King, 2003; Mascari et al., 2016; OECD/NEA/CSNI, 2017). Previously at OSU, the H2TS method was adopted to design the APEX facility to develop a representative thermal–hydraulic database of AP600 to validate safety analysis computer codes (Reyes and Hochreiter, 1998).

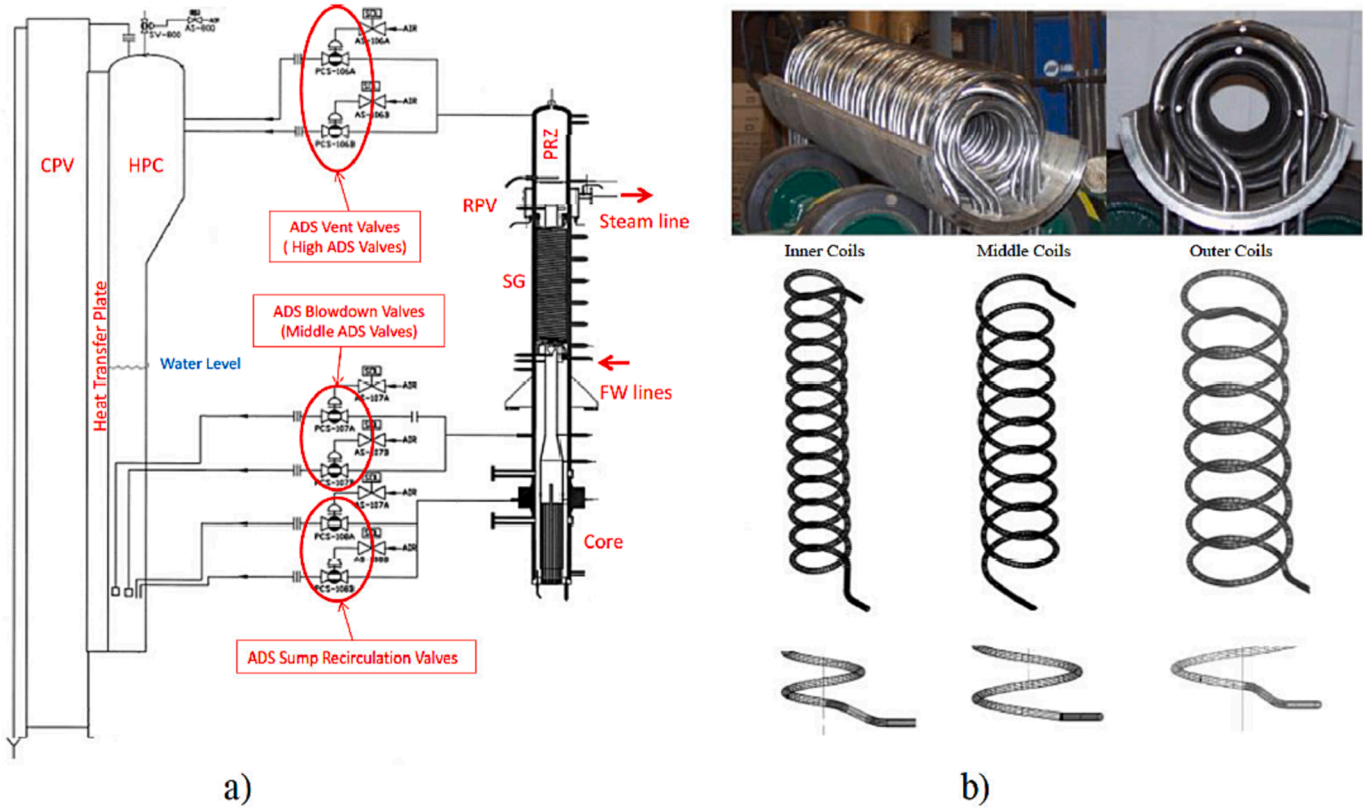


**Fig. 1.** a) Schematic diagram of the RPV, containment structures and the RPV/HPC connection of the OSU-MASLWR experimental facility and b) helical coil sg bundle (Mascari et al., 2019).

Fig. 1 a) shows a schematic diagram of the RPV, containment structures and the RPV/High Pressure Containment (HPC) connections of the OSU-MASLWR experimental facility. The facility is constructed entirely of stainless steel, and is designed for full pressure and full temperature prototypical operation. It includes the primary circuit, consisting of the RPV and Automatic Depressurization System (ADS) lines, the secondary circuit and the containment structures.

The internal components of the RPV are the core, the hot leg riser, the upper plenum, the pressurizer, the SG primary side, the cold leg downcomer and the lower plenum. The core has 56 cylindrical heater rods distributed in a 1.86 cm pitch square array, with a 1.33 pitch to diameter ratio. The nominal power of each heater rod is 7.1 kW resulting in a maximum core power of 398 kW. The diameter of the core rod is 1.59 cm. A lower core flow plate contains 76 auxiliary flow holes of 0.635 cm of diameter, arranged at 1.86 cm pitch square array, and 57 core rod flow holes.

The secondary circuit includes the Feed Water (FW) treatment and storage system, the main FW pump, the main FW system supply lines, the SG secondary side internal to the vessel, the main steam system and associated FW and steam valves. The SG of the facility is a once through heat exchanger and is located within the RPV in the annular space between the hot leg riser and the inner surface of the RPV. The tube bundle is a helical coil consisting of fourteen tubes (Fig. 1 b). There are three separate parallel coils of stainless steel tubes. The outer and middle coils consist of five tubes each while the inner coil consists of four tubes.

The HPC consists of a lower cylindrical section, a concentric cone section, an upper cylindrical section and a hemispherical upper head. The Cooling Pool Vessel (CPV) consists of a tall right cylindrical tank. One rupture disk connects the HPC and the CPV and a heat transfer plate is located between them. A total of six ADS lines (two high ADS lines, two middle ADS lines and two ADS sump recirculation lines) connect the RPV to the HPC. A more detailed description of the facility can be found in (Reyes and King, 2003; Mascari et al., 2012c; Mascari et al., 2016).

### 2.2. OSU-MASLWR test 002

OSU-MASLWR test 002 is a natural circulation test that investigated the primary system flow rate and secondary side steam superheat for a variety of core power levels and SG FW flow rates. The test stepped power level incrementally from lower power up to 165 kW, varying the SG FW flow rate at each power level. The main phenomena of interest in this test are (Mascari et al., 2016; IAEA, 2014; OECD/NEA/CSNI, 1996a, OECD/NEA/CSNI, 1996b; IAEA, 2009; IAEA, 2012):

- RPV:
  - o Single phase natural circulation;
  - o Heat transfer in covered core;
  - o Distribution of pressure drop through primary system;
  - o Direct heat exchange between riser and downcomer (by pass heat transfer (Mascari et al., 2016; Mascari et al., 2011b; IAEA, 2014));
  - o Heat transfer in SG primary side;

  Structural heat[1] and heat losses.

- RPV-SG:
  - o Heat transfer in SG secondary side;
  - o Steam superheated on secondary side.

In general, the level of the steam superheat is changed to control the facility. Since the slope of the main steam superheat curve increases if the value of the core power increases and decreases if the value of the FW flow rate increases, the target of these tests was to acquire primary system flow rate and secondary side steam superheat for different core powers and FW flow rates.

[1] Energy stored in the metallic structures.

## 3. TRACE code and OSU-MASLWR facility nodalization

### 3.1. TRACE code

The TRACE code is a best-estimate thermal–hydraulic system code developed by the USNRC (U. S. Nuclear Regulatory Commission, 2013). It is a component-oriented code developed for best-estimate analysis for LWRs. In particular, TRACE was designed for the simulation of operational transients, LOCAs and to model the thermal–hydraulic phenomena taking place in the experimental facilities used to study the steady state and transient behavior of reactor fission systems. The code is based on two fluid, two-phase field equations with a semi-implicit or stability enhancing two-step (SETS) numerical solution scheme. Detailed information on TRACE code can be found in (Mascari et al., 2016; Mascari et al., 2011a; Mascari et al., 2012b; U. S. Nuclear Regulatory Commission, 2013; Bersano et al., 2020).

In the present study TRACE V5 patch 4 was used. The nodalization has been developed using SNAP.

### 3.2. OSU-MASLWR facility nodalization

The OSU-MASLWR TRACE nodalization (Fig. 2) has been developed throughout several years in SNAP, with a continuous update following the code development (Mascari et al., 2016; Mascari et al., 2008; Mascari et al., 2011a; Mascari et al., 2011b; Mascari et al., 2012a; Mascari et al., 2012b; Mascari et al., 2019; IAEA, 2014; Pottorf et al., 2009). The nodalization models the primary and the secondary circuit, the HPC, the heat transfer plate and the CPV. The ADS blowdown lines, vent lines and sump recirculation lines are modelled as well. The "slice nodalization" technique is adopted to improve the capability of the code to reproduce natural circulation phenomena. This technique considers mesh cells of different nodalization zones at the same elevation and with the same cell length. In this way, errors due to the position/elevation of the cell nodalization center that can influences the results of the calculated data when natural circulation regime is present are reduced (Mascari et al., 2012b).

The primary circuit of the TRACE model is composed by the core, the hot leg riser, the upper plenum, the pressurizer, the SG primary side, the cold leg downcomer and the lower plenum. From the top of the hot leg riser, the flow enters in the upper plenum which is divided into two thermal hydraulic regions connected to the pressurizer. After the upper plenum, the flow continues downward through the SG primary section and into the cold leg downcomer region. The core is modelled with one thermal hydraulic region thermally coupled with one equivalent active heat structure simulating the 56 electric heaters. The pressurizer is modelled with two hydraulic regions, connected by a set of single junctions, to allow the simulation of potential natural circulation/convection phenomena. The three different PRZ heater elements are modelled with one equivalent active heat structure. The thick baffle plate is modelled as well. The direct heat exchange by the internal shell between the hotter fluid in the hot leg riser and the colder fluid in the descending annular downcomer is modelled by heat structures thermally coupled with these two different hydraulic regions.

The SG coils are modelled with one "equivalent" series of pipes thermally coupled by an equivalent heat structure with the SG primary side section. The "curved pipe" option, available from TRACE v5 patch 4, has been activated in the inner hydraulic cells of the SG to model the helical coil heat transfer.

The RPV, HPC and CPV shell and the connected insulation are modelled. In particular, the HPC is modelled with one hydraulic region connected by a heat structure, representing the heat transfer plate, to the CPV simulated with another hydraulic region. The ADS lines are modelled separately, considering also the heat losses. RPV, HPC and CPV shell and the connected insulation are modelled.

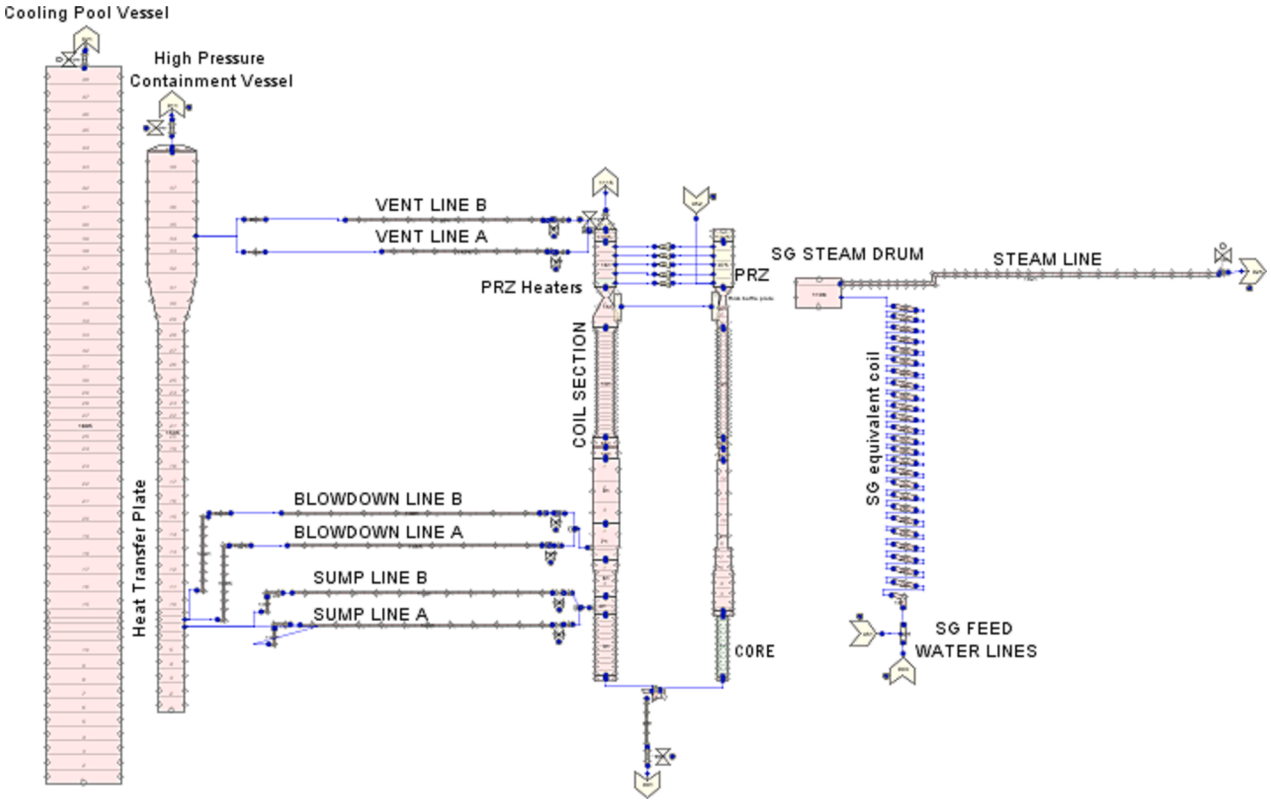


**Fig. 2.** OSU-MASLWR facility TRACE nodalization (developed through SNAP).

## 4. Methodology

### 4.1. Scaling-up approach

The scale-up of the TRACE input-deck has been performed in two subsequent steps (Fig. 3):

1. Height scaling (scaling factor 3);
2. Flow area scaling (scaling factor 254.7/3).

In the height scaling, it has been scaled by the length of all hydrodynamic components and heat structures, the core power and the SG FW mass flow rate.

In the flow area scaling, starting from the height scaled model, it has been scaled up by the flow area and hydraulic diameter of all hydrodynamic components, both the vertical and the horizontal ones (except for the hydraulic diameter of the core and the secondary side SG tubes, since they are considered to have prototypical dimensions and therefore it is increased their multiplicity). Heat structure diameters and thicknesses were scaled according to the approach presented in (Petelin et al., 2007) preserving the hoop tensile stress. The geometry of core heaters and SG tubes heat structures has been maintained as in the base model, increasing the number of rods and tubes respectively according to the scale factor. Also, in this case the core power and the SG FW mass flow rate have been scaled. Table 1 summarizes the different models adopted for the scaling analysis.

In addition to the comparison of significant thermal–hydraulic parameters, in order to evaluate the results of the scaling procedure, the characteristic time constant and selected non-dimensional numbers have been evaluated along the transient. In particular (Reyes, 2005; Reyes and King, 2003):

- Characteristic time constant:

$$\tau_{loop} = \sum_{i=1}^{N} \frac{l_i}{u_i} = \sum_{i=1}^{N} \tau_i = \frac{M_{sys}}{\dot{m}} = \frac{M_{sys}}{\rho_l u_c a_c} \tag{1}$$

- Loop Richardson Number:

$$\prod_{Ri} = \frac{\beta g (T_H - T_c) L_{th}}{u_c^2} \tag{2}$$

- SG Heat Transport Number:

$$\prod_{SG} = \frac{\dot{q}_{SG}}{\dot{q}_{Core}} \tag{3}$$

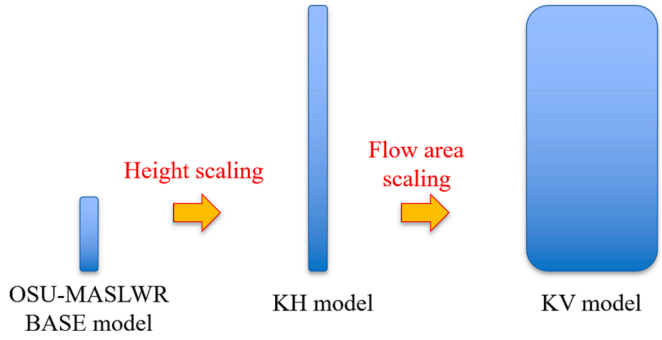


**Fig. 3.** Scaling steps and related models.

**Table 1**
Summary of the performed calculations.

| Calculation | Label | Description |
|---|---|---|
| Base model | BASE | The nodalization geometrical parameters and boundary conditions correspond to the OSU-MASLWR facility and Test 002. |
| Height scaled model | KH | Starting from the BASE model, the length of all hydrodynamic components and heat structures have been increased by a factor of 3. In order to preserve the thermal–hydraulic conditions, the core power and the SG FW mass flow rate has been increased by the same factor; this allows to preserve the mass and energy ratio. |
| Volume scaled model | KV | Starting from the KH model, the flow area and hydraulic diameter of all hydrodynamic components (except for the hydraulic diameter of the core and the secondary side SG tubes), the number of core rods and SG tubes have been increased by a factor of 254.7/3. In order to preserve the thermal–hydraulic conditions, the core power and the SG FW mass flow rate has been increased by the same factor; this allows to preserve the mass and energy ratio. Heat structure diameters and thicknesses were scaled to preserve the hoop tensile stress |

- Loop Heat Loss Number:

$$\prod_{Loss} = \frac{\dot{q}_{loss}}{\dot{q}_{Core}} \tag{4}$$

where $l$ is the length of the i-th section, $u$ the fluid velocity, $M_{sys}$ the primary loop fluid mass, $\dot{m}$ the mass flow rate, $\rho$ the density, $a$ the flow area, $\beta$ is the thermal expansion coefficient, $g$ is the gravity constant, $T$ is the temperature, $L_{th}$ is the distance between heat source and heat sink thermal centers and $\dot{q}$ is the power. The Richardson Number has been calculated considering the velocity $u_c$ at the inlet of the core, the core outlet temperature $T_H$ and the core inlet temperature $T_C$. Since in the base model orifices are present at the core inlet, in the KH model the orifice flow areas have been scaled to preserve the Richardson Number. Assuming that $\beta$, $g$ and $(T_H - T_c)$ should remain constant since the fluid is at prototypical conditions, the term $L_{th}/u_c^2$ should be preserved in the Base and KH models. Considering that the ratio of $L_{th}$ and of the mass flow rate is 3 in the height scaling, it follows that the flow area of the single orifice is scaled by $\sqrt{3}$.

### 4.2. Accuracy evaluation

The accuracy of the code results has been evaluated for both the base model and the scaled-up ones. The accuracy evaluation has been performed in two steps:

1. Qualitative accuracy evaluation
2. Quantitative accuracy evaluation

The qualitative accuracy evaluation is a subjective judgment by the code user of the calculated results considering the capability of the code to predict the involved phenomena based on the behavior of the selected parameters. This is done by identifying the Phenomenological Windows (PhWs) of the test and examining the associated relevant thermal–hydraulic phenomena of interest. Then, a subjective judgment for each phenomenon is given, through a visual comparison of the experimental and calculated results. More details on the adopted accuracy evaluation methodology can be found in (Mascari et al., 2016).

In the present study, the qualitative accuracy evaluation is based on four subjective judgment marks (Excellent (+), Reasonable (o), Minimal (NA), Unqualified (-)), which are assigned both to the experimental and the calculated data. Table 2 shows the meaning of the experimental and calculated data qualitative judgement marks.

The quantitative accuracy evaluation is a procedure that gives a

**Table 2**
Judgement marks for the qualitative accuracy evaluation (Mascari et al., 2016).

| Data | + | o | NA | - |
|---|---|---|---|---|
| Experimental | Phenomenon occurred in the test and it is directly measured | Phenomenon occurred in the test and it is indirectly measured | Phenomenon occurred during the test but there is no instrumentation to detect (lack of instrumentation) | Phenomenon not occurred in the test |
| Calculated | Phenomenon is clearly predicted by the code (**Excellent**) | Phenomenon is partially predicted (i.e. the answer of the code is **reasonable** but closure code relations are not appropriate, etc.) | Models are not appropriate to predict (i.e. nodalization strategy, etc.) (**Minimal**) | Phenomenon is not predicted by the code (**Unqualified**) |

numerical indication of the performance of a calculation. In this analysis, it has been carried out through the FFTBM (Ambrosini et al., 1990). In this method, it is computed the difference between the calculated and the experimental data, which is then passed to the frequency domain using the Fast Fourier Transform. The accuracy evaluation is then performed on the resulting Average Amplitude (AA) and the Weighted Frequency (WF) (Prošek et al., 2008; Prošek and Leskovar, 2015). The AA is usually adopted as a measure of the code accuracy; the lower is the AA, the more accurate is the result. The WF gives an information about the frequencies that more significantly contribute to the discrepancies between the calculated data and the experimental ones. The accuracy evaluation is mainly based on the AA parameter, while the WF is an additional qualitative information that may be considered for the accuracy evaluation (Ambrosini et al., 1990).

Starting from the AA and the WF calculated for each parameter selected for the accuracy evaluation, the total AA and the total WF can be computed using proper weighting factors. In the present study the weighting factors have been considered equal to one for all parameters. Apart from the choice of the weighting factors, the FFTBM has been applied in a default way with a cut-off frequency of 0.4 Hz. The tool adopted to perform the FFTBM analysis is the JSI FFTBM Add-In 2007 developed at Jožef Stefan Institute (Slovenia) (Prošek, 2007; Prošek et al., 2008; Prošek and Leskovar, 2015). The reference threshold values for the AA for the accuracy evaluation are taken as in (D'Auria et al., 1999). For the scaled-up calculations, the experimental data of powers, levels and flow rates have been scaled according to the scaling factor.

## 5. Results

### 5.1. Thermal-hydraulic parameters

The first analysis conducted to evaluate the scaling process is to compare relevant thermal–hydraulic parameters resulting from the three calculations (BASE, KH and KV) against the OSU-MASLWR test 002 experimental data. Temperatures and pressures have been directly compared, whereas the proper scaling factor has been applied to power, flow rates and collapsed levels.

Fig. 4 (left) shows the core power in the three different models (scaled by the proper factor). The agreement with the experimental data in each power step is due fact that the core power is imposed through a POWER component connected to the Heat Structure simulating the core heaters according to the experimental results. Fig. 4 (right) shows the primary side volumetric flow rate in the hot leg riser. The calculated results of the three models (scaled by the proper factor) agree with the experimental data, considering the proper scaling factor. It should be underlined that the agreement of the mass flow rate is an important result considering that the natural circulation in the RPV is the target phenomenon of this study.

Fig. 5 shows the core inlet (left) and outlet (right) temperatures of the three models against the experimental data. The calculated results are all in agreement with the experimental data and the temperature behavior along the transient is predicted. Similarly, also the primary coolant temperature at the top of the chimney (Fig. 6 left) and after the SG coils (Fig. 6 right) agree among the three models and with the experimental data. During the test, different core power and SG feedwater values are investigated. The slight increment or reduction of the primary temperatures may be due to the balance between the core power and the SG removed power in the various steps of the test.

The pressurizer pressure (Fig. 7 left) agrees between the three models and the experimental data. The level in the pressurizer of the base model agrees with the experimental data; moreover, also the level in the KH and KV calculations is in agreement considering the experimental data multiplied by the height scaling factor.

Considering the secondary side, the SG FW mass flow rate is shown in Fig. 8 (left) and the inlet pressure is shown in Fig. 8 (right). The agreement of the FW mass flow rate (scaled by the proper factor) and inlet pressure is due to the fact that they are imposed according to the experimental data, considering the proper scaling factor in the KH and KV calculations for the mass flow rate. Similarly, the SG FW inlet temperature, Fig. 9 (left), is imposed according to the experimental data and therefore agrees among the three models.

Fig. 9 (right) shows the calculated SG secondary side outlet mixture temperature of the three calculations that agrees with the experimental data, even if some oscillations are present in the BASE model at the end of the transient and in the KV model at the beginning of transient, due to the income of saturated fluid. In addition, the main steam pressure (Fig. 10) agrees among the three models and with the experimental data.

In conclusion, from a visual observation of the selected parameters, they all result to be qualitatively and quantitatively comparable considering the proper scaling factor, when needed.

In addition to the comparison of relevant thermal–hydraulic parameters resulting from the three calculations against the OSU-MASLWR test 002 experimental data, it has been also compared the RPV and SG temperature diagrams resulting from the three calculations. In particular, Fig. 11 shows the results at 1900s. Considering the RPV temperature diagram, the temperature increases almost linearly in the core region, then it slightly decreases in the riser due to the heat transfer between the riser region and the SG primary side/downcomer regions, see by pass heat transfer in Section 2.2. Then the primary temperature reduces in the primary side of the SG, due to the heat transfer to the secondary side, and finally slightly increases in the downcomer due to the by pass heat transfer (Section 2.2). Concerning the SG temperature diagram, the primary side temperature gradually reduces due to the heat transfer towards the secondary side. For the secondary side it is possible to observe the subcooled region, with the fluid temperature lower than the saturation one, the saturated region with a constant temperature and the superheated region above the saturation temperature.

From a visual observation, the RPV and SG temperature profiles result to be qualitatively and quantitatively comparable. A slight difference is present on the location where the superheat begins within the SG tubes (in this analysis at higher elevations in KH and KV calculations with respect to the Base one), but the final superheating is comparable in the three cases.

### 5.2. Accuracy evaluation

The accuracy of the three calculations has been evaluated considering the methodology presented in Section 4.2. Initially, the qualitative accuracy evaluation has been performed judging the capability of the code to predict the involved phenomena in the three calculations. As

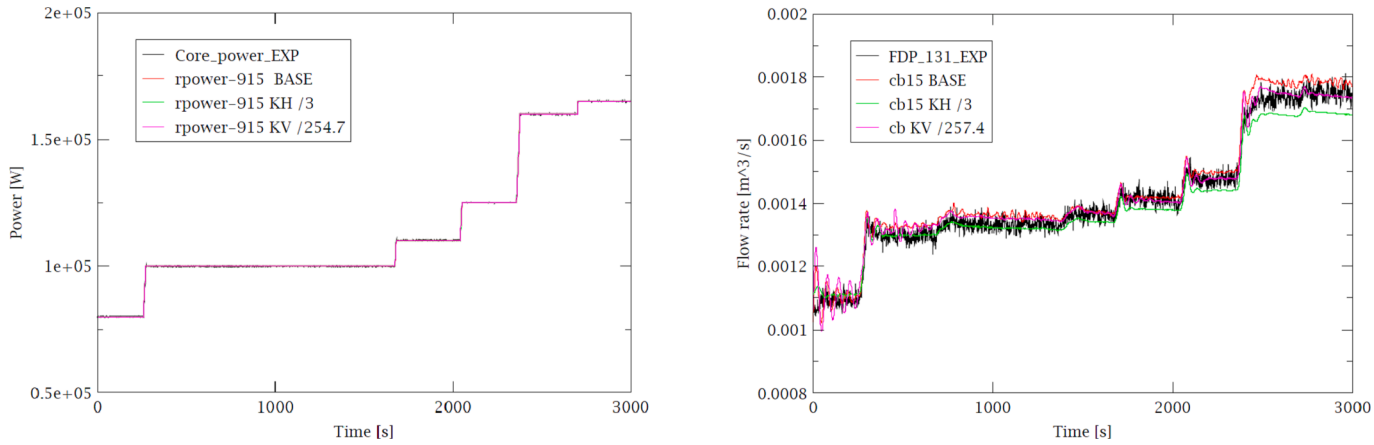


**Fig. 4.** Core power (left) and primary volumetric flow rate (right).

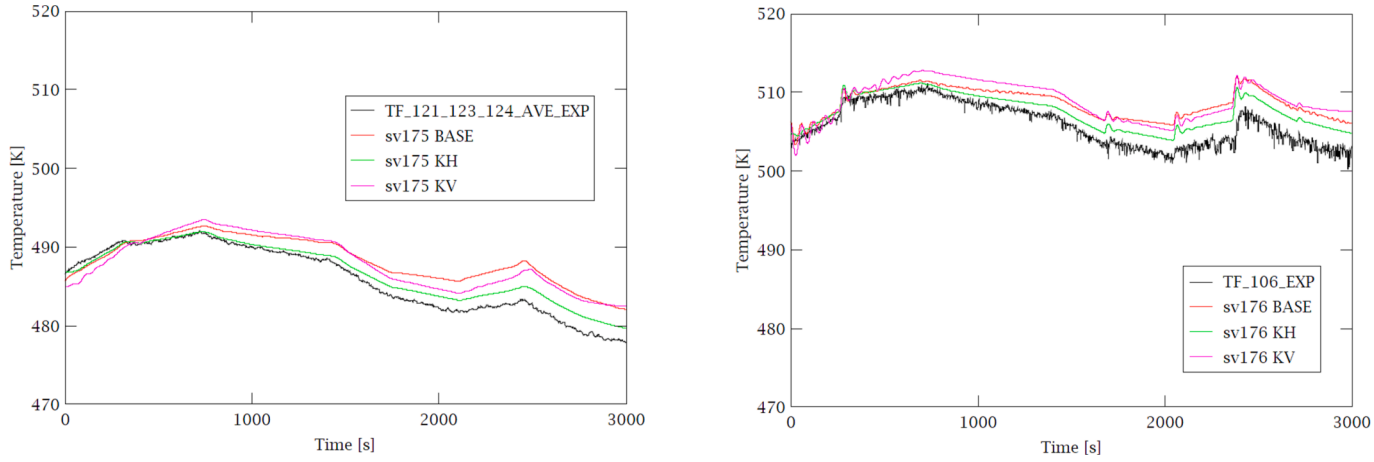


**Fig. 5.** Core inlet (left) and outlet (right) temperature.

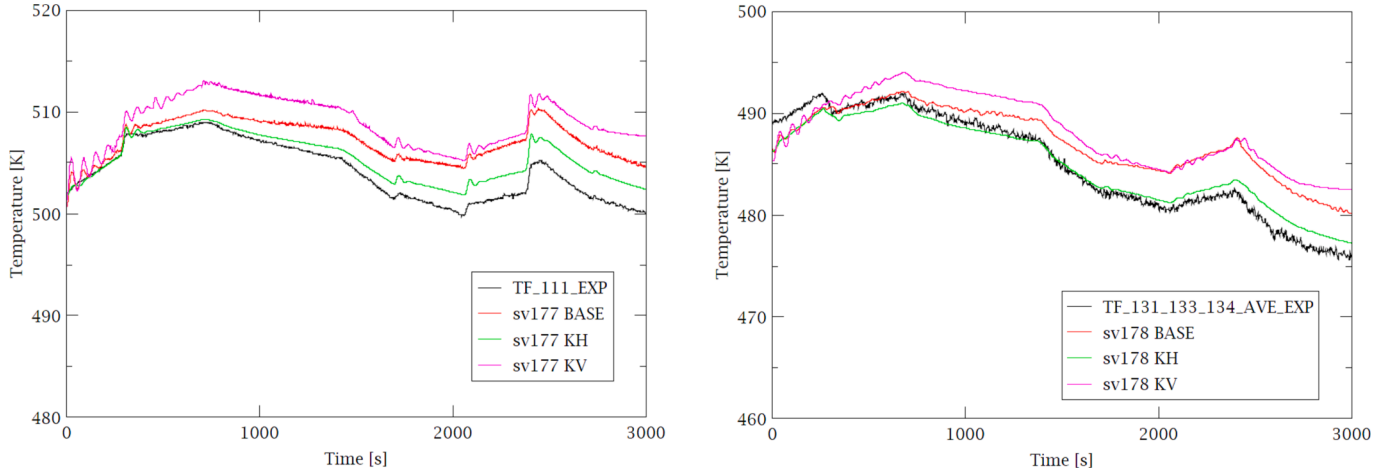


**Fig. 6.** Primary coolant temperature at the top of the chimney (left) and after the SG coils (right).

shown in Table 3, all the three models are able to predict the thermal–hydraulic phenomena observed in the OSU-MASLWR test 002.

After the qualitative accuracy evaluation, a quantitative analysis was performed applying the FFTBM considering the PhW from (Mascari et al., 2019). As shown in Table 4, all the AA values are below the threshold of 0.3 identifying a very good code accuracy for each parameter according to (D'Auria et al., 1999). As previously mentioned, the AA is adopted as a measure of the code accuracy; the lower the AA is, the more accurate the result is. Moreover, it has been compared the AA of the various models and the accuracy of the scaled-up calculations (KH and KV) resulted in similar accuracy compared to the base calculation.

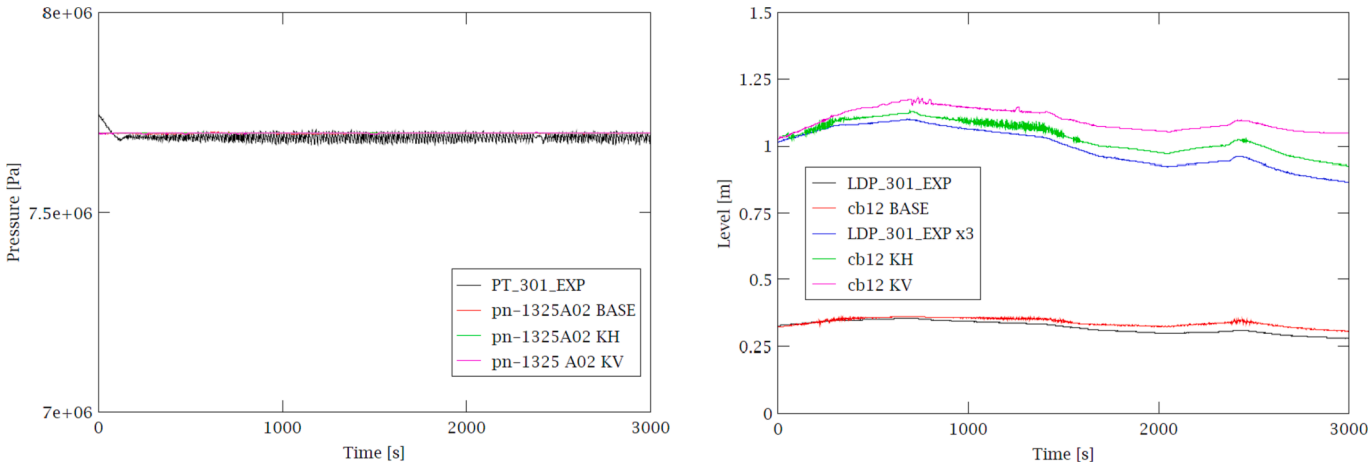


**Fig. 7.** Pressurizer top pressure (left) and collapsed water level (right).

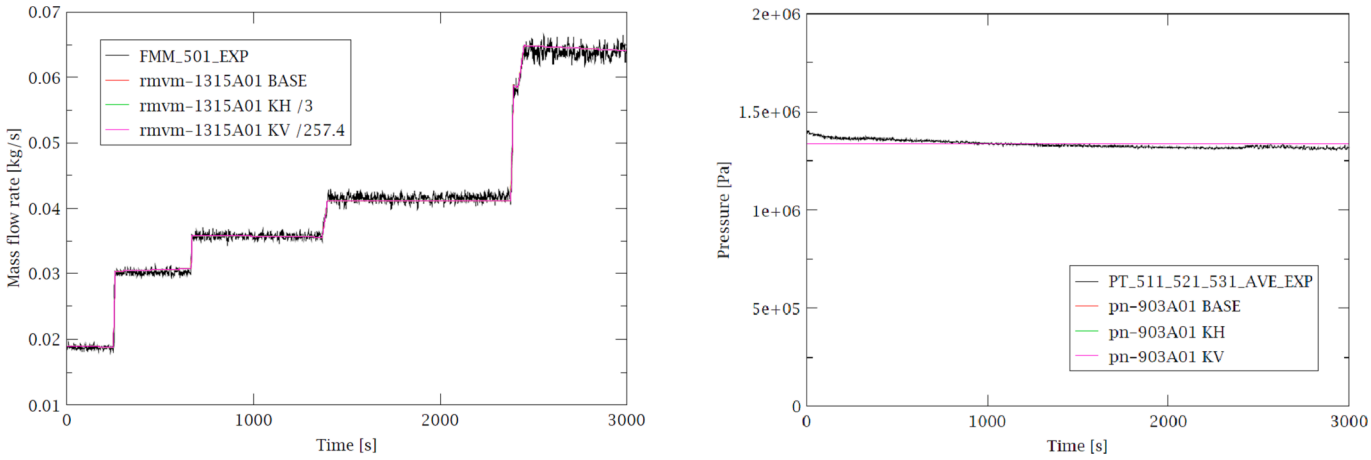


**Fig. 8.** SG FW mass flow rate (left) and inlet pressure (right).

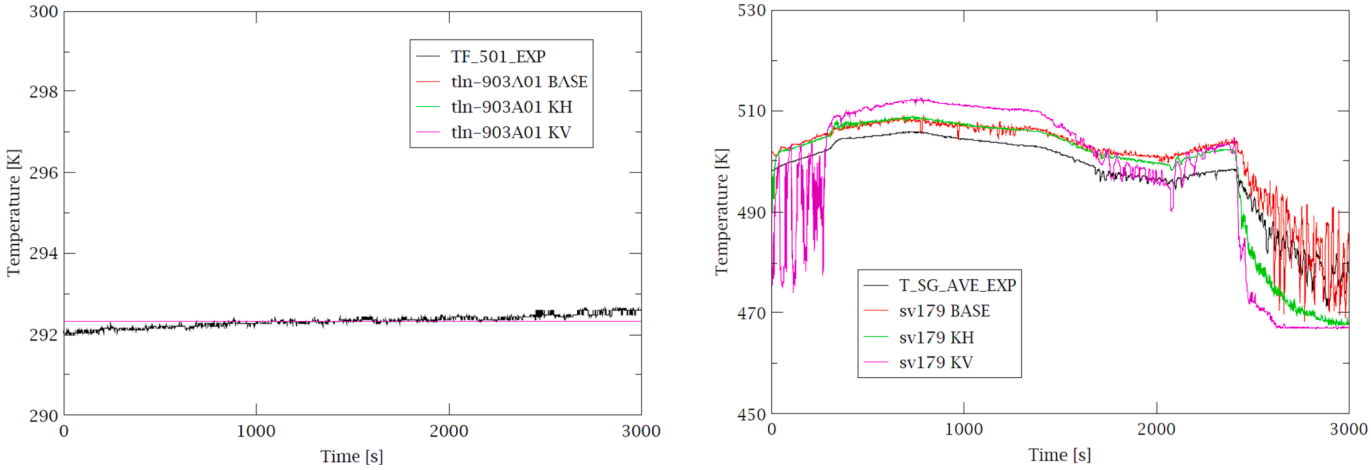


**Fig. 9.** SG FW inlet temperature (left) and secondary side outlet temperature (right).

### 5.3. *Characteristics and non-dimensional numbers*

To evaluate the results of the scaling process, relevant characteristic and non-dimensional numbers have been considered to verify if they are preserved in the two scaling steps. Fig. 12 shows the loop characteristic time constant (left) and Richardson number (right). For both numbers, the results agree among the three models and the quantitative value is correctly predicted in the various power steps.

The SG heat transport number and loop heat loss number are shown in Fig. 13. The SG heat transport number agrees among the three calculations, even if oscillations are present in all the results. The oscillations seem to be caused by the calculated tube-side heat transfer

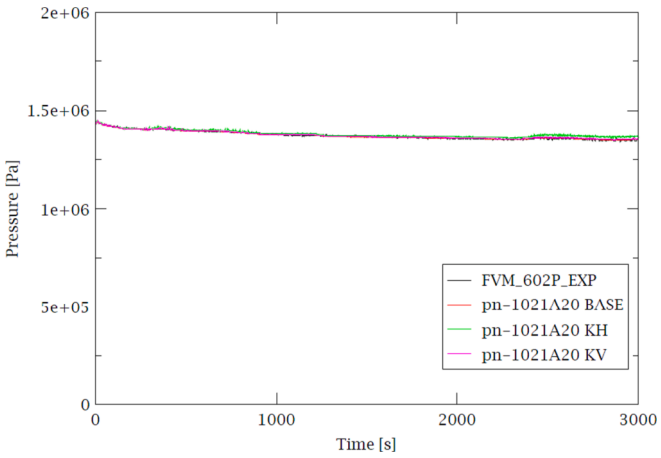


**Fig. 10.** Main steam pressure.

To quantitatively characterize the discrepancies of the characteristic and non-dimensional numbers in the scaling process the FFTBM has been applied. In this case experimental data are not available, therefore the results of the BASE calculation have been considered as reference values. The results of the FFTBM application are reported in Table 5. The loop time constant and the Richardson number have an AA below 0.4. The SG heat transport number high AA is due to the oscillations observed in the calculated results with all models.[2] However, the visual analyses shows that the SG number is consistent in the three calculations. The heat loss number has a low AA in the KH calculation, while the relative high AA in the KV calculation is due to the missing preservation of this number as already mentioned in the qualitative analysis.

## 6. Conclusions

Following the validation activity of the TRACE code against the OSU-MASLWR experimental tests, the numerical scaling of the OSU-MASLWR TRACE input deck has been performed against natural circulation test

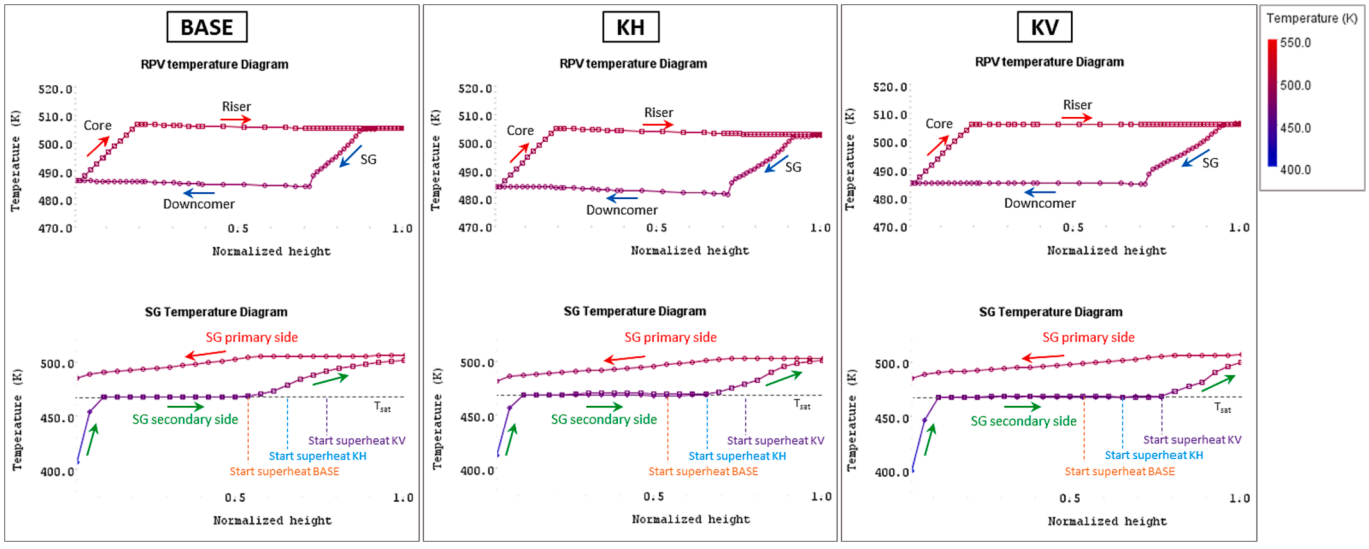


**Fig. 11.** RPV and SG temperature diagram of the BASE (left), KH (center) and KV (right) calculations at 1900s.

**Table 3**
Qualitative accuracy evaluation results.

| Phenomenon | Experiment | | TRACE BASE | TRACE KH | TRACE KV |
|---|---|---|---|---|---|
| | Phenomena | Measurement | Phenomena | Phenomena | Phenomena |
| Single-phase Natural Circulation | + | + | + | + | + |
| Heat Transfer in Covered Core | + | + | + | + | + |
| By Pass Heat Transfer | + | + | + | + | + |
| Distribution of Pressure Drop Through Primary System | + | + | + | + | + |
| Heat Transfer in SG Primary Side | + | + | + | + | + |
| Structural Heat and Heat Losses | + | o | + | + | + |
| Heat Transfer in SG Secondary Side | + | + | + | + | + |
| Steam Superheated on Secondary Side | + | + | + | + | + |

coefficient that influence the SG power (numerator of the SG heat transport number). The loop heat loss number agrees between the Base and KH calculations since the outer heat transfer surface increases with the scaling factor, because the height of the heat structures is augmented. In the KV calculation, the heat loss number is not preserved since the outer heat transfer surface does not increase linearly with the scale factor. In particular, the external heat transfer area per fluid volume for the heat losses is lower in the KV model compared to the Base and KH ones.

[2] In relation to the adoption of the FFTBM method, it is to underline that the presence of oscillations in the different calculated data could give relatively high values of AA, even if the curves, from a visual observation, seem in reasonable agreement. These oscillations in fact can introduce higher frequencies that in principle could be not physical but add spurious contribution in the AA computation increasing its value. Therefore, in a validation process for safety review purpose, more detailed analysis could be necessary to analyze the nature of the oscillations, both in the experimental and/or calculated signals, and by investigating the AA values as a function of the cut-off frequency.

**Table 4**
Quantitative accuracy evaluation results (AA).

| Variables[1] | PhW 0 – 250 s | | | PhW 250 – 667 s | | | PhW 667 – 1370 s | | | PhW 1370 – 2378 s | | | PhW 2378 – 3060 s | | |
|---|---|---|---|---|---|---|---|---|---|---|---|---|---|---|---|
| | BASE | KH | KV | BASE | KH | KV | BASE | KH | KV | BASE | KH | KV | BASE | KH | KV |
| Core_power | 0.01 | 0.01 | 0.01 | 0.02 | 0.02 | 0.02 | 0.01 | 0.01 | 0.01 | 0.01 | 0.01 | 0.01 | 0.07 | 0.07 | 0.07 |
| TF121_123_124_AVE | 0.00 | 0.00 | 0.01 | 0.01 | 0.00 | 0.01 | 0.01 | 0.00 | 0.01 | 0.02 | 0.01 | 0.01 | 0.01 | 0.01 | 0.01 |
| TF106 | 0.01 | 0.01 | 0.01 | 0.01 | 0.01 | 0.02 | 0.02 | 0.01 | 0.02 | 0.03 | 0.03 | 0.03 | 0.03 | 0.03 | 0.03 |
| TF131_133_134_AVE | 0.01 | 0.01 | 0.01 | 0.01 | 0.01 | 0.02 | 0.01 | 0.01 | 0.02 | 0.02 | 0.01 | 0.02 | 0.02 | 0.01 | 0.02 |
| TF111 | 0.01 | 0.00 | 0.01 | 0.01 | 0.00 | 0.01 | 0.01 | 0.00 | 0.01 | 0.02 | 0.01 | 0.02 | 0.01 | 0.01 | 0.02 |
| FDP_131 | 0.24 | 0.18 | 0.27 | 0.17 | 0.14 | 0.19 | 0.20 | 0.18 | 0.19 | 0.20 | 0.20 | 0.20 | 0.19 | 0.19 | 0.18 |
| PT301 | 0.01 | 0.01 | 0.01 | 0.01 | 0.01 | 0.01 | 0.02 | 0.02 | 0.02 | 0.02 | 0.02 | 0.02 | 0.02 | 0.02 | 0.02 |
| LDP301 | 0.07 | 0.06 | 0.05 | 0.10 | 0.07 | 0.12 | 0.15 | 0.12 | 0.12 | 0.20 | 0.12 | 0.19 | 0.18 | 0.08 | 0.24 |
| FMM501 | 0.12 | 0.12 | 0.12 | 0.13 | 0.13 | 0.13 | 0.15 | 0.15 | 0.15 | 0.20 | 0.20 | 0.20 | 0.15 | 0.15 | 0.15 |
| PT511_521_531_AVE | 0.08 | 0.08 | 0.08 | 0.06 | 0.06 | 0.06 | 0.06 | 0.06 | 0.06 | 0.05 | 0.05 | 0.05 | 0.06 | 0.06 | 0.06 |
| TF501 | 0.00 | 0.00 | 0.00 | 0.00 | 0.00 | 0.00 | 0.00 | 0.00 | 0.00 | 0.00 | 0.00 | 0.00 | 0.00 | 0.00 | 0.00 |
| T_SG_AVE | 0.01 | 0.03 | 0.14 | 0.01 | 0.01 | 0.08 | 0.02 | 0.01 | 0.02 | 0.03 | 0.02 | 0.05 | 0.13 | 0.09 | 0.11 |
| FVM_602P | 0.01 | 0.01 | 0.01 | 0.02 | 0.03 | 0.02 | 0.03 | 0.03 | 0.03 | 0.02 | 0.03 | 0.02 | 0.03 | 0.06 | 0.04 |
| Total | **0.05** | **0.04** | **0.06** | **0.04** | **0.04** | **0.05** | **0.05** | **0.05** | **0.05** | **0.06** | **0.05** | **0.06** | **0.07** | **0.06** | **0.07** |

Core_power: core thermal power; TF121_123_124_AVE: core inlet average temperature; TF106: core outlet temperature; TF131_133_134_AVE: downcomer average temperature (after SG); TF111: chimney top temperature; FDP_131: primary volumetric flow rate (at chimney); PT301: pressurizer pressure; LDP301: pressurizer water level; FMM501: SG FW mass flow rate; PT511_521_531_AVE: SG FW average pressure; TF501: SG FW temperature; T_SG_AVE: SG average secondary side outlet temperature; FVM_602P: main steam pressure.

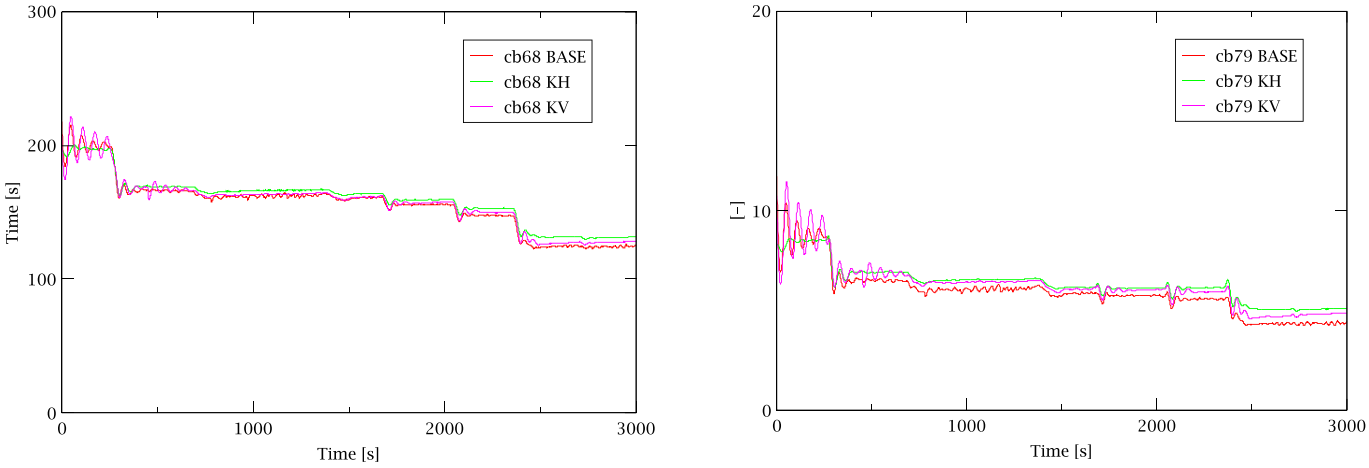


**Fig. 12.** Loop characteristic time constant (left) and Richardson number (right).

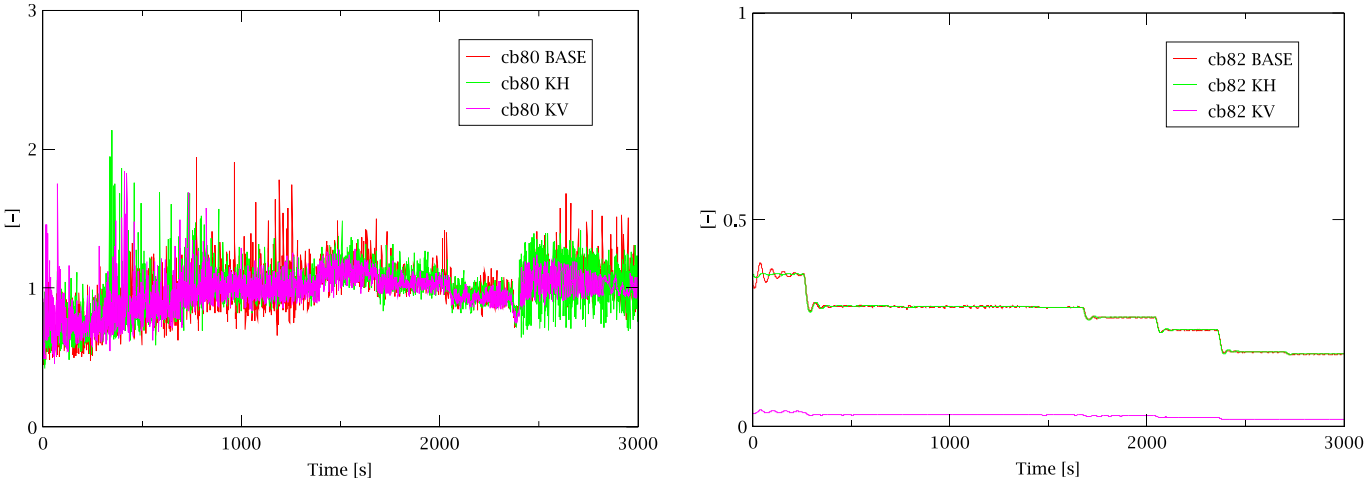


**Fig. 13.** SG heat transport number (left) and loop heat loss number (right).

002. The qualitative analyses show that the important phenomena are predicted by the code in the different scaled configurations (Base, KH, KV). The FFTBM has been applied to evaluate the quantitative accuracy of the base and scaled-up models. The accuracy of the thermal–hydraulic parameters of the scaled-up calculations (KH and KV) resulted similar to the accuracy of the base calculation.

**Table 5**
FFTBM results of the characteristics and non-dimensional numbers (AA).

| Variables | PhW 0 – 250 s | | PhW 250 – 667 s | | PhW 667 – 1370 s | | PhW 1370 – 2378 s | | PhW 2378 – 3060 s | |
|---|---|---|---|---|---|---|---|---|---|---|
| | KH | KV | KH | KV | KH | KV | KH | KV | KH | KV |
| Loop Time Constant | 0.16 | 0.12 | 0.06 | 0.07 | 0.07 | 0.06 | 0.08 | 0.05 | 0.10 | 0.08 |
| Richardson Number | 0.40 | 0.27 | 0.15 | 0.16 | 0.17 | 0.16 | 0.22 | 0.16 | 0.23 | 0.19 |
| SG Heat Transport Number | 0.87 | 1.07 | 1.16 | 0.99 | 0.90 | 0.85 | 0.72 | 0.63 | 1.00 | 0.71 |
| Heat Loss Number | 0.13 | 0.90 | 0.03 | 0.91 | 0.05 | 0.91 | 0.02 | 0.90 | 0.05 | 0.91 |
| Total | 0.39 | 0.59 | 0.35 | 0.53 | 0.30 | 0.50 | 0.26 | 0.44 | 0.35 | 0.47 |

Relevant characteristics such as the characteristic time constant, and non-dimensional numbers have been considered to assess the scaling process. In general, they are preserved between the base and scale-up models and this is also quantitatively confirmed applying the FFTBM. In the flow area scaling the heat loss number is not preserved since the outer heat transfer surface does not scale linearly with the core power. In addition, the SG heat transport number resulted to have a high AA value in both scale–up models. This is due to the oscillatory behavior of the parameters that can led to some limitation in a standard application of the FFTBM. However, from a visual observation the SG heat transport number agrees between the three calculations from a qualitative point of view.

The confirmation of the scalability of the TRACE RPV nodalization gives some first insights on the current capability of the TRACE code to scale-up the natural circulation plant behavior. A full evaluation of the TRACE code scale-up capability would require the assessment of all the implemented correlations in different transient scenarios; therefore, further analyses are in progress considering the available experimental data, to have an exhaustive code scale-up scalability assessment. Moreover, other type of tests (e.g., blowdown test 001) may be considered to extend the code scalability assessment to the primary/containment coupling phenomena typical of iPWR. The discussed approach allows also to use the best estimate thermal–hydraulic system code as extrapolation tool (Mascari et al., 2015) to scale-up experimental data developed in scaled-down facilities.

## CRediT authorship contribution statement

**Fulvio Mascari:** Writing – original draft, Supervision, Resources, Methodology, Investigation, Formal analysis, Conceptualization. **Andrea Bersano:** Writing – original draft, Visualization, Methodology, Investigation, Formal analysis, Conceptualization. **Brian G. Woods:** Writing – review & editing. **Jose N. Reyes:** Writing – review & editing. **Kent Welter:** Writing – review & editing. **Hideo Nakamura:** Writing – review & editing.

## Declaration of competing interest

The authors declare that they have no known competing financial interests or personal relationships that could have appeared to influence the work reported in this paper.

## Data availability

The authors are unable or have chosen not to specify which data has been used.

## Acknowledgments

The authors gratefully wish to acknowledge the support and advice of Prof. Francesco D'Auria in the development of the activity described in this paper. In addition, the authors gratefully acknowledge USNRC for their valuable comments and suggestions during the preparation of the manuscript.

ENEA carried out the research activity with TRACE code and SNAP, obtained in the framework of the ENEA-ISIN agreement signed on March 23rd 2020 as part of the General Arrangement between the United States Nuclear Regulatory Commission (US-NRC) and the Italian National Inspectorate for Nuclear Safety and Radiation Protection (ISIN).

## References

Ambrosini, W., Bovalini, R., D'Auria, F., 1990. Evaluation of accuracy of thermalhydraulic code calculation. Energia Nucleare 7, 5–16.
Applied Programming Technology, Inc., 2021, "Symbolic Nuclear Analysis Package (SNAP) User's Manual".
Bersano, F., Mascari, M.T., Porfiri, P., Maccari, C.B., 2020. Ingress of Coolant Event simulation with TRACE code with accuracy evaluation and coupled DAKOTA Uncertainty Analysis. Fusion Eng. Des. 159.
Bovalini, R., D'Auria, F., De Varti, A., Maugeri, P., Mazzini, M., 1992. Analysis of counterpart tests performed in boiling water reactor experimental simulators. Nucl. Technol. 97 (1).
Chung, Y.J., Lim, S.W., Bae, K.H., 2014. Investigation of TASS/SMR Capability to Predict a Natural Circulation in the Test Facility for an Integral Reactor. Science and Technology of Nuclear. Installations.
D'Auria, F., Debrecin, N., Galassi, G.M., Galeazzi, S., 1993. Application of Relap5/Mod3 to the evaluation of loss of feedwater in test facilities and in nuclear plants. Nucl. Eng. Des. 141 (3).
D'Auria, F., Debrecin, N., Galassi, G.M., 1995. Outline of the uncertainty methodology based on accuracy extrapolation (UMAE). Nucl. Technol. 109 (1).
D'Auria, F., Cherubini, M., Galassi, G.M., Muellner, N., 2005. Analysis of measured and calculated counterpart test data in PWR and VVER1000 simulators. J. Nucl. Technol. Radiat. Protect. 1.
F. D'Auria, M. Frogheri, W. Giannotti, 1999, RELAP/MOD3.2 Post Test Analysis and Accuracy Quantification of SPES Test SP-SB-04, NUREG/IA-0155.
F. D'Auria, 1992, "Scaling and counterpart tests", *OECD/NEA/CSNI Specialist Meeting on Transient Two-Phase Flow - Current Issues in System Thermal Hydraulics.*
IAEA, 2009, TECDOC-1624, *Passive safety systems and natural circulation in water cooled nuclear power plants.*
IAEA, 2012, TECDOC-1677, *Natural circulation phenomena and modelling for advanced water cooled reactors.*
IAEA, 2014, TECDOC-1733, *Evaluation of advanced thermohydraulic system codes for design and safety analysis of integral type reactors.*
F. Mascari, F. De Rosa, B. G. Woods, K. Welter, G. Vella, F. D'Auria, 2016, *Analysis of the OSU-MASLWR 001 and 002 Tests by Using the TRACE Code*, NUREG/IA-0466.
Mascari, F., Woods, B.G., Adorni, M., 2008. Analysis, by TRACE code, of Natural Circulation Phenomena in the MASLWR-OSU-002 test. Proceedings of the International Conference Nuclear Energy for New Europe 2008.
Mascari, F., Vella, G., Woods, B.G., 2011a. TRACE Code Analyses for the IAEA ICSP on Integral PWR Design Natural Circulation Flow Stability and Thermo-Hydraulic Coupling of Containment and Primary System during Accidents. Proceedings of the ASME 2011 Small Modular Reactors Symposium, September 28-30, 2011, Washington, DC, USA.
Mascari, F., Vella, G., Woods, B.G., Welter, K., Pottorf, J., Young, E., Adorni, M., D'Auria, F., 2011b. Sensitivity analysis of the MASLWR helical coil steam generator using TRACE. Nucl. Eng. Des. 241, 1137–1144.
Mascari, F., Richiusa, M.L., Vella, G., Woods, B.G., Welter, K., D'Auria, F., 2012a. Analysis of the OSU-MASLWR-003A Natural Circulation Test by Using the TRACE Code. Advances In Thermal Hydraulics (ATH '12) Conference, November 11–15, 2012, San Diego California.
Mascari, F., Vella, G., Woods, B.G., Welter, K., D'Auria, F., 2012b. Analysis of primary/containment coupling phenomena characterizing the MASLWR design during a SBLOCA Scenario. Nuclear Power Plants. InTech.
Mascari, F., Vella, G., Woods, B.G., D'Auria, F., 2012c. Analyses of the OSU-MASLWR Experimental Test Facility. Science and Technology of Nuclear. Installations.
Mascari, F., Nakamura, H., Umminger, K., De Rosa, F., D'Auria, F., 2015. Scaling Issues for the Experimental Characterization of Reactor Coolant System in Integral Test Facilities and Role of System Code as Extrapolation Tool. Proceedings Of International Topical Meeting on Nuclear Reactor Thermal Hydraulics 2015 (NURETH 2015), 30 August – 4 September 2015, USA.
Mascari, F., Woods, B.G., Welter, K., D'Auria, F., 2019. Validation of the TRACE code against Small Modular Integral Reactor natural circulation phenomena. Proceedings

of 2018 International Topical Meeting on Nuclear Reactor Thermal Hydraulics (NURETH18).
Mascari, F., Bersano, A., Woods, B.G., Reyes, J.N., Welter, K., Nakamura, H., D'Auria, F., 2022. Scaling-up capabilities of TRACE integral reactor nodalization against natural circulation phenomena in Small Modular Reactors. Proceedings of the 19th International Topical Meeting on Nuclear Reactor Thermal Hydraulics (NURETH-19).
Mascari, F., Woods, B.G., Welter, K., D'Auria, F., Bersano, A., Maccari, P., 2023. Small modular reactors and insights on passive mitigation strategy modeling. Nucl. Eng. Des. 401, 112088.
Modro, S.M., Fisher, J.E., Weaver Jr., K.D., Reyes, J.N., Groome, J.T., Babka, P., Carlson, T.M., 2003. Multi-application small light water reactor final report. DOE Nuclear Energy Research Initiative Final Report. Idaho National Engineering and Environmental Laboratory.
OECD/NEA/CSNI, 1996a, *CSNI integral test facility validation matrix for the assessment of thermal-hydraulic codes for LWR LOCA and transients*, NEA/CSNI/R(96)17.
OECD/NEA/CSNI, 1996b, *Relevant thermal hydraulic aspects of advanced reactor design, Status Report*, OCDE/GD(97)8, NEA/CSNI/R(1996)22.
OECD/NEA/CSNI, 2017, *A State-of-the-art Report on Scaling in System Thermal Hydraulics Applications to Nuclear Reactor Safety and Design*, NEA/CSNI/R(2016)14.
Petelin, S., Mavko, B., Koncar, B., Hassan, Y.A., 2007. Scaling of the small-scale thermal hydraulic transient to the real nuclear power plant. Nucl. Technol. 158, 56–68.
Pottorf, J., Mascari, F., Woods, B., 2009. TRACE, RELAP5 Mod 3.3, and RELAP5-3D code comparison of OSU-MASLWR-001 test. Trans. Am. Nucl. Soc. 101.
Prošek, M.L., 2015. Use of FFTBM by signal mirroring for sensitivity study. Ann. Nucl. Energy 76, 253–262.
Prošek, M., Leskovar, B.M., 2008. Quantitative assessment with improved fast Fourier transform based method by signal mirroring. Nucl. Eng. Des. 238, 2668–2677.
Prošek, 2007, "JSI FFTBM Add-In 2007 User's Manual", IJS-DP-9752.
Reventós, F., Batet, L., Llopis, C., Pretel, C., Salvat, M., Sol, I., 2007. Advanced qualification process of ANAV NPP integral dynamic models for supporting plant operation and control. Nucl. Eng. Des. 237, 2014–2023.
Reventos, F., Martinez-Quiroga, V., Freixa, J., 2019. Perfecting the use of hybrid models in scaling analysis. Nucl. Eng. Des. 354 (1).
Reyes Jr., J.N., 2003. Scaling analysis for the OSU integral system test facility. Department of Nuclear Engineering Oregon State University 116 Radiation Center Corvallis, OR 97331–5902 NERI Project 99–0129. Prepared For U.S Department of Energy.
Reyes Jr., J.N., 2005. Integral system experiment scaling methodology, Annex 11, Natural circulation in water cooled nuclear power plants phenomena, models, and methodology for system reliability assessments. In: IAEA-TECDOC-1474 Annex 11, pp. 321–356.
Reyes Jr., J.N., Groome, J., Woods, B.G., Young, E., Abel, K., Yao, Y., Yoo, J.Y., 2007. Testing of the multi application small light water reactor (MASLWR) passive safety systems. Nucl. Eng. Des. 237, 1999–2005.
Reyes, J.N., Hochreiter, L., 1998. Scaling analysis for the OSU AP600 test facility (APEX). Nucl. Eng. Des. 186 (1–2), 53–109.
U. S. Nuclear Regulatory Commission, 2013, "TRACE V5.840 Theory Manual, Field Equations, Solution Methods and Physical Models".